Using Linear Systems Theory to Study Nonlinear Dynamics of Relay Cells

Rahul Agarwal and Sridevi V. Sarma

Institute for Computational Medicine, Johns Hopkins University, 3400 N Chrles Street, Baltimore, U.S.A.

Keywords: Relay Neurons, Thalamus, Reliability, Hodgkin Huxley Type Models.

Abstract: Relay cells are prevalent throughout sensory systems and receive two types of inputs: driving and modulating. The driving input contains receptive field properties that must be relayed while the modulating input alters the reliability of this relay. In this paper, we analyze a biophysical based nonlinear model of a relay cell and use systems theoretic tools to construct analytic bounds on how well the cell transmits a driving input as a function of the neuron's electrophysiological properties, the modulating input, and the driving signal parameters. Our analysis applies to both 2nd & 3rd order model as long as the neuron does not spike without a driving input pulse and exhibits a refractory period. Our bounds suggest, for instance, that if the frequency of the modulating input increases and the DC offset decreases, then reliability increases. Our analysis also shows how the biophysical properties of the neuron (e.g. ion channel dynamics) define the oscillatory patterns needed in the modulating input for appropriately timed relay of sensory information.

1 INTRODUCTION

Relay neurons are found in various brain nuclei including the thalamus (Samuel et al., 2004; Hirsch et al., 1983; Seki et al., 2003). Experiments have suggested that the inputs to a relay neuron can be divided into two categories: driving and modulating. The driving input is made up of few synapses on the proximal dendrites whereas the modulating input comprises all other synapses (Guillery and Sherman, 2002) (see Figure 1). The relay neuron processes and relays information in the driving input, conditioned on the modulating input.(Sherman and Guillery, 1998; Sherman, 2007). For example, the lateral geniculate nucleus (LGN) in the thalamus receives the driving input from the retina and modulating input from cortex. The function of the LGN is to selectively relay information from the retina to primary visual cortex (Guillery and Sherman, 2002; O'Connor et al., 2002).

In this study we rigorously analyze biophysical based models of relay neurons and characterize the nonlinear electro-physiological dynamics of a single relay cell as a function of the cell type and the inputs. Various attempts to study relay neurons are made in (Rubin and Terman D., 2004; Masson et al., 2002; Guo et al., 2008; Wolfart et al., 2005; Rubin and Josic K, 2007). These studies also suggest that the relay neuron's reliability is governed by the modulating input combined with the intrinsic properties of the neuron, however the results were shown to be true for only few realizations of modulating and driving input. The work presented here is an extension of the work we presented in (Agarwal and Sarma, 2011) where we employ systems theoretic tools to obtain an explicit analytical bounds on reliability for a 2nd order model. In this work we showed that same methodology can also be employed to obtain bounds on 3rd order model as long as the neuron does not spike without a pulse in the driving input and exhibits a refractory period. Consequently, our analysis is relevant for relay cells whose electrophysiological dynamics, including bursting, may be governed by several different ion channels and is more rigorous than previous works. Our bounds predict the dependence of relay reliability as a function of the neuron's electrophysiological properties (i.e., model parameters), the modulating input signal, and the driving signal parameters. Our lower and upper bounds suggests, for example, that if the frequency of the modulating input increases and/or its DC offset decreases, then relay reliability increases.

2 MATERIALS AND METHODS

In this section, first we describe a biophysical model of a relay neuron, and then use systems theoretical tools to compute bounds on relay reliability.

2.1 A Relay Neuron Model

A relay neuron receives two kinds of inputs: a driving input, $r(t)$ and a modulating input $u(t)$, and generates one output, $V(t)$, as shown in Figure 1.

Below is a state space representation of 3rd order Hodgkin-Huxley type biophysical model of a relay neuron. This model was used in (Guo et al., 2008; Rubin and Terman D., 2004), which is a simplification of model used in (Sohal and Huguenard, 2002; Sohal et al., 2000). The response of the model for an oscillating modulating input and a Poisson driver input is also shown in Figure 1.

$$\dot{\mathbf{x}} = \mathbf{f}(\mathbf{x}) + \begin{pmatrix} -u(t) & 0 & 0 \\ 0 & 0 & 0 \\ 0 & 0 & 0 \end{pmatrix} \mathbf{x} + \begin{pmatrix} r(t) \\ 0 \\ 0 \end{pmatrix}, \quad (1)$$

where $\mathbf{f}(\mathbf{x}) =$

$$\begin{pmatrix} -(I_L + I_{Na} + I_K + I_T) + I_{ext} \\ \frac{(h_\infty(X_1 + V_{syn}) - X_2)}{(\tau_h(X_1 + V_{syn}))} \\ \frac{(r_\infty(X_1 + V_{syn}) - X_2)}{(\tau_r(X_1 + V_{syn}))} \end{pmatrix}. \quad (2)$$

Here $I_L = g_L(V - V_L)$, $I_{Na} = g_{Na} m_\infty^3 h(V - V_{Na})$, $I_K = g_L(0.75(1 - h))^4(V - V_L)$ are the leak current, sodium and potassium current respectively. $I_T = g_T p_\infty^2(V) r(V - V_T)$ and I_{ext} are the low threshold potassium current and external current respectively. All the parameters used are same as those in (Guo et al., 2008) and are given in the table 1.

In general, a state space representation takes the form $\dot{\mathbf{x}} = \mathbf{f}(\mathbf{x}, \mathbf{r}, \mathbf{u})$, however, there is more structure in (1). From (1), one can see that $\mathbf{f}(\mathbf{x})$ is only a function of the system's internal states. The modulating input, $u(t)$, multiplies the first component of the state $\mathbf{x}$, while the driving input, $r(t)$, is an exogenous input to the system.

2.1.1 Inputs and Outputs

For our analysis, we assume that the driving input belongs to class of delta pulse train with Poisson arrivals, i.e. $r(t) = I_0 \sum_{i=1}^{n} \delta(t - \tau_i)$. The $\tau_i's$ are generated randomly such that $\tau_{i+1} = \tau_i + T_0 + \tau'$, where $T_0 \in \mathbb{R}$ is a constant that represents the refractory period of driving input, and $\tau' \in \mathbb{R}^+$ is exponentially distributed
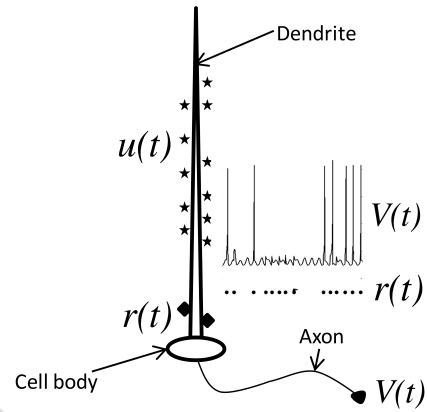

Figure 1: **A Relay Neuron** - Illustrating a relay neuron. Ensemble activity of all the distal synapses (stars) is modulating input $u(t)$. The proximal synapses (diamonds) form driving input $r(t)$. The output is axonal voltage $V(t)$. The inset plots the voltage profile obtain from the model in response to pulses in $r(t)$. Note that each pulse in $r(t)$ may or may not generate a spike.

with rate λ. Therefore, the average inter-pulse interval is $T = E(\tau_{i+1} - \tau_i) = T_0 + 1/\lambda$. We assume that the modulating input belongs to set of sinusoidal function i.e. $u(t) = c_1 + c_2 sin(\omega t)$. The output of the relay neuron is membrane voltage $V(t) = x_1(t) + V_{syn}$. Details of all the parameters and reasons for the chosen classes for driving and modulating input can be found in (Agarwal and Sarma, 2011).

2.1.2 Properties of the Model

Finally, the function $\mathbf{f}(\mathbf{x})$ is assumed to have the following properties but is otherwise general:

1. **Stable Neuron.** Consider (1) with $u(t) = c_1$ and $r(t) = 0$,. In general, this system may have multiple equilibria with different stability properties. But for our purposes, we choose $\mathbf{f}(\mathbf{x})$ such that (1) with $u(t) = c_1, r(t) = 0$ has only one globally stable **equilibrium point**, $\bar{\mathbf{x}}$, for all pragmatic c_1. Such a neuron is called a **stable neuron** (Manor et al., 1997). This condition ensures that the neuron does not have any limit cycle, therefore, the neuron does not spike without a pulse in $r(t)$.

This further implies that if a small periodic modulating input is applied to a stable neuron (1), $u(t) = c_1 + c_2 sin(\omega t), r(t) = 0$, then after a sufficient amount of time the system's state vector will lie within a small neighbourhood of the equilibrium point. However, the state vector never reaches $\bar{\mathbf{x}}$ due to the time varying modulating input. The trajectory of the state in this neighbourhood can be solved using linearization methods and is periodic (Agarwal and Sarma, 2011). We define this periodic trajectory as **the steady state**

orbit of a stable neuron, $\mathbf{x_o}(\mathbf{t})$. See Figure 2 A.

Next, we define $\mathbb{X}_\infty$ as the collection of all points in the steady state orbit. If the initial state of the system $x(t = 0) \notin \mathbb{X}_\infty$ then $\mathbb{X}_\infty$ is not achievable in finite time. Therefore, we relax our definition to the collection of all points inside a tube of ε thickness around the steady state orbit, and define this tube as the set $\mathbb{X}_r$, i.e.

$$\mathbb{X}_r = \{\mathbf{x} \in \mathbb{R}^n | \; \|\mathbf{x} - \mathbf{v}\| \leq \varepsilon \text{ for a } \mathbf{v} \in \mathbb{X}_\infty\}. \quad (3)$$

2. **Threshold Behaviour.** To define threshold behaviour of a neuron, we first define a **successful response**. A successful response at time t is a change in V such that $V(t) > -50mV$ & $V(t - \tau) \leq -50mV$ $\forall \tau \in (0, L)ms$. Note that both a single spike or a burst of spikes, with intra burst interval less than L ms, are counted as a successful response under this definition. We use this definition so that we can extend our analysis to bursty neurons characterized by higher order models.

Almost all stable neurons show a threshold behaviour (Platkiewicz and Brette R, 2010; Lodish et al., 2000).

Now, we define $x_{th} = V_{th} - V_{syn}$, where V_{th} is the traditional threshold voltage for generating a successful response (Platkiewicz and Brette R, 2010; Lodish et al., 2000; FitzHugh, 1955). In (Platkiewicz and Brette R, 2010) it has been shown that spike threshold is influenced by ion channels activation and synaptic conductance. In our case we assume a constant threshold for simplicity. We show in results section that our analytical bounds calculated using this assumption contained the relay performance obtained by doing simulations on the original model. Finally, we define the **threshold current, I_{th}**, such that $\bar{x}_1 + I_{th} = x_{th}$. Note, by definition both I_{th} and V_{th} have the same units and hence can be added.

Illustrations of a successful response, unsuccessful response, I_{th}, V_{th}, x_{th} $\mathbb{X}_\infty$, $\mathbb{X}_r$ are shown in Figure 2 A B, C, for a second order system. Note that, I_{th} and V_{th} are functions of c_1, since different values of c_1 result in different $\mathbf{F}(\mathbf{x})$. This dependence is a linear function i.e $I_{th}(c_1) \simeq I_{th}(0) + mc_1$.

2.2 Response to Pulses in $r(t)$

When a reference pulse arrives, there are 2 possible responses of system in (1). The neuron either gives a **successful response** or **unsuccessful response**. In Figure 2 C, we have plotted these two types of responses.

It is straightforward to see how these two responses occur. The reference pulse causes the state

vector to " jump" to $\mathbf{x}(t_i) = \mathbf{x}(t_i^-) + [I_0, 0]^T$. This is easy to show by direct integration of (1), on the time interval $\lim_{\Delta t \to 0}[t_i - \Delta t, t_i]$. If the dynamics of x_2, x_3, are slow and $x_1(t_i) > x_{th} - I_0$ (see Figure 2 A,B) the neuron will generate a successful response, otherwise it will return back to the equilibrium point generating unsuccessful response. Now, we define set $\mathbb{X}_s$ as the collection of points in $\mathbb{X}_r$ whose first component $x_1 > x_{th} - I_0$. These points result in successful response after a pulse in $r(t)$. Similarly we define $\mathbb{X}_{us} \subseteq \mathbb{X}_r$ as the collection of points whose first component $x_1 \leq x_{th} - I_0$, hence these points result in unsuccessful spikes after a pulse in $r(t)$. These sets are illustrated in Figure 2 A. Note that if the reference pulse does not occur for a T_r time interval i.e, the system state will move into $\mathbb{X}_r$.
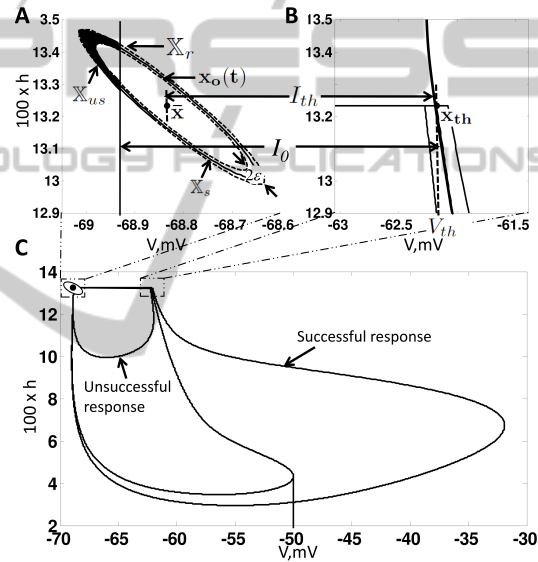

Figure 2: **Properties of $\mathbf{f}(\mathbf{x})$** - **(A)** Illustrates the equilibrium point $\bar{\mathbf{x}}$, the steady state orbit $\mathbf{x_o}(t)$ and the orbit tube, $\mathbb{X}_r$, for $\mathbf{f}(\mathbf{x})$ for a second order neuron. **(B)** Illustrates $\mathbf{x_{th}}$, the threshold voltage V_{th} and threshold current I_{th}. Note that these parameters are defined by the undriven system $u(t) = c_1, r(t) = 0$. **(C)**Illustrates a successful response trajectory and an unsuccessful response trajectory.

2.3 Relay Reliability

We define relay reliability as:

$$R \triangleq Pr(\text{Successful spike due to a reference pulse }). \quad (4)$$

Using (4) and definition of $\mathbb{X}_s$, we can write:

$$R = Pr\left(X(t^-) \in \mathbb{X}_s | r(t) = I_0\delta(0)\right) \quad (5a)$$

$$= Pr\left(X(t_i) \in \mathbb{X}_s\right) \text{ for any } i = 1, 2, \cdots. \quad (5b)$$

Noting $\mathbb{X}_s \subseteq \mathbb{X}_r$, we break (5b) as:

$$R = Pr(X(t_i) \in \mathbb{X}_s \& \mathbb{X}_r) \tag{6a}$$

$$= Pr(X(t_i) \in \mathbb{X}_r) Pr(X(t_i) \in \mathbb{X}_s | X(t_i) \in \mathbb{X}_r) \tag{6b}$$

$$\triangleq P_{pulse} \times P_{spike}. \tag{6c}$$

Here we have used the definition of conditional probability (Greenstied and Snell, 2003) to go from (6b) to (6c). Although not explicit in (6), relay reliability is a function of the driver input parameters, I_0 and T, the modulating input parameters, c_1, c_2, and ω, and the neuron's dynamics (i.e. model parameters) denoted by H. In the next section, we compute closed-form approximations of lower and upper bounds of reliability as a function of I_0, T, c_2, c_1, ω and H, by computing P_{spike} and bounds on P_{pulse}.

2.4 Calculation of P$_{spike}$

We have already calculated P_{spike} for a second order model and is same as R in (Agarwal and Sarma, 2011). The exact analysis can be repeated for the 3rd order models and P_{spike} can be estimated as the ratio of time spent by the state trajectory in $\mathbb{X}_s$ and $\mathbb{X}_{us}$ given it is in $\mathbb{X}_r$. This gives:

$$P_{spike} = \frac{\pi + 2 sin^{-1}\left(\frac{I_0 - I_{th}}{c_2 |H_1(j\omega)|\bar{x}_1}\right)}{2\pi}. \tag{7}$$

Here $H_1(j\omega) = \frac{1}{2\pi} \int h_1(t) e^{-j\omega t} dt$ is the transfer function of the neuron $x_1(t) - \bar{x}_1 = h_1 * u(t)$. Details of the above expression can be found in (Agarwal and Sarma, 2011).

2.5 Calculation of P$_{pulse}$ & R

In this section, we compute P_{pulse} to ultimately obtain an expression for R. Since a driver pulse that arrives at time t_i can only result in either a successful spike or an unsuccessful spike, we can equivalently write the definition of P_{pulse} as:

$$P_{pulse} = Pr(\mathbf{x}(t_i) \in \mathbb{X}_r | \text{ SR at } t_{i-1}) \cdot Pr(\text{SR at } t_{i-1})$$
$$+ Pr(\mathbf{x}(t_i) \in \mathbb{X}_r | \text{ USR at } t_{i-1}) \cdot Pr(\text{ USR } t_{i-1}). \tag{8a}$$

Here, we have used the law of total probability and the definition of conditional probability (Greenstied and Snell, 2003) to arrive at (8a). We know that after a successful spike at t_{i-1}, the system state $X(t) \notin \mathbb{X}_r$, only for $t \in (t_{i-1}, t_{i-1} + T_r)$. Therefore, we see that

$$Pr(X(t_i) \in \mathbb{X}_r | \text{ SR at } t_{i-1}) = Pr(t_i - t_{i-1} \geq T_r). \tag{9}$$

Similarly, if T_r^{us} denotes time to resting tube after unsuccessful spike, then we get:

$$Pr(X(t_i) \in \mathbb{X}_r | \text{ USR at } t_{i-1}) = Pr(t_i - t_{i-1} \geq T_r^{us}). \tag{10}$$

As T_r^{us} has complex dependence upon input and model parameters it is hard to calculate $Pr(t_i - t_{i-1} \geq T_r^{us})$. However, it is certain that $T_r^{us} \leq T_r$. This implies that $Pr(t_i - t_{i-1} \geq T_r) \leq Pr(t_i - t_{i-1} \geq T_r^{us})$, by properties of cumulative distributive functions (Greenstied and Snell, 2003). Therefore, we get the following bounds:

$$Pr(t_i - t_{i-1} \geq T_r) \leq Pr(t_i - t_{i-1} \geq T_r^{us}) \leq 1 \tag{11}$$

Putting together (8a),(9),(10) and (11), we get:

$$P_{pulse} \geq R \cdot Pr(t_i - t_{i-1} \geq T_r) \tag{12a}$$

$$+ (1-R) \cdot Pr(t_i - t_{i-1} \geq T_r) \tag{12b}$$

$$\text{and } P_{pulse} \leq R \cdot Pr(t_i - t_{i-1} \geq T_r) + (1-R). \tag{12c}$$

Now we calculate $Pr(t_i - t_{i-1} \geq T_r)$. Recall that the inter pulse intervals of $r(t)$, $t_i - t_{i-1} = \tau + T_0$, here τ is generated from an exponential distribution and T_0 is refractory period. Therefore:

$$Pr(t_i - t_{i-1} \geq T_r) = Pr(T_0 + \tau \geq T_r) \tag{13a}$$

$$= Pr(\tau \geq T_r - T_0) \tag{13b}$$

$$= \int_{T_r - T_0}^{\infty} f_\tau(\tau) d\tau \triangleq \alpha. \tag{13c}$$

It can be easily shown that:

$$\alpha = \begin{cases} e^{\frac{-(T_r - T_0)}{T - T_0}} & T_r - T_0 \geq 0 \\ 1 & T_r - T_0 < 0 \end{cases}. \tag{14}$$

Here T is the average inter pulse interval, $E(t_i - t_{i-1})$. Finally, by combining (12c) and (13) we get:

$$\alpha \leq P_{pulse} \leq 1 - R(1-\alpha). \tag{15a}$$

Now we compute bounds on relay reliability i.e $R_l \leq R \leq R_u$ as:

$$\frac{P_{spike}}{1 + (1-\alpha)P_{spike}} \geq R \geq \alpha \cdot P_{spike}. \tag{16}$$

From (16) and (13), one can see that if $T >> T_r$, then $R_l \to R_u \to P_{spike}$. This result is intuitive because if pulses in $r(t)$ occur at a slow rate, then the solution of (1) has enough time to return to the orbit tube after each pulse. Therefore, $P_{pulse} \triangleq P(X(t) \in X_r) \to 1$ and hence $R \to P_{spike}$.

3 RESULTS

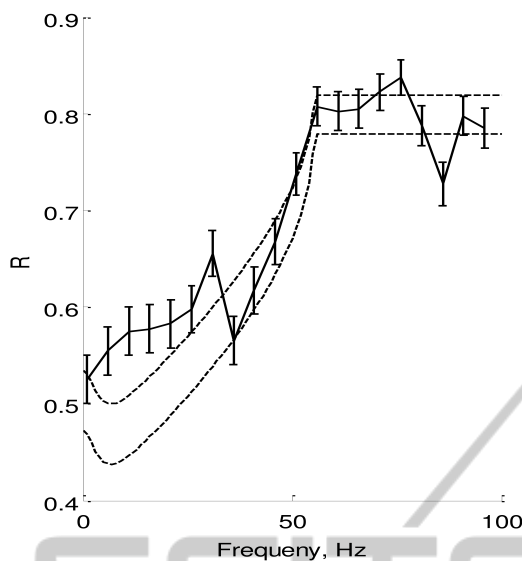In this section, we will apply (16) to (1).

Figure 3: R vs $\frac{\omega}{2\pi}$ for the 3rd order model - Plots theoretical and numerically computed reliability versus $\frac{\omega}{2\pi}$, with $c_2 = 0.015, c_1 = 0.075, I_0 = 6.5, T_r = 105ms, T_0 = 80ms, T = 180ms$. Dotted lines are lower and upper bounds on reliability from the (16). Solid line is plotting R_{emp} calculated by running simulation of (1), error bars show $\pm std$. We estimated $I_{th} = 6$ as the minimum hieght of a $r(t)$ pulse, that make the neuron spike.

In Figure 3, we plot our reliability bounds (16) along with reliability computed numerically through simulation of the 3rd order model. We see that our bounds predict the reliability well except for some errors in the low frequency range. This is due to the fact that we did not consider higher order dynamics of the 3rd order model. However, our bounds qualitatively predict the trend of reliability well even for the higher order model.

In general, our analytical bounds are applicable to higher dimensional models as long as the model 1. does not generate a spike if there is no pulse in $r(t)$, and 2. has a threshold behavior. The second condition is true for most of neurons that satisfy the first condition. Our analysis may also be extended to include neurons that spike without any driver input, but in this manuscript we neglect such dynamics.

4 DISCUSSION

In this manuscript, we studied the reliability of a relay neuron. A relay neuron receives two inputs: a driving input, $r(t)$, and a modulating input, $u(t)$. The neuron generates one output, $V(t)$, which relays $r(t)$ conditioned on $u(t)$. Our goal was to precisely determine how the modulating input impacts relay reliability. To

calculate relay reliability, we used LTI systems theoretic tools to derive the analytical bounds (16) on relay reliability as a function of different input and model parameters. Specifically, (16) implies that if the modulating input is of the form $u(t) = c_1 + c_2 sin(\omega t)$, then increasing c_1 or c_2 decreases reliability. However, increasing ω increases reliability. In addition, our reliability curve (see Figure 3) suggests that on increasing ω, reliability first increases slowly and then increases rapidly and plateaus. (16) is powerful as it characterizes the multiple dependencies of reliability on $u(t), r(t)$ and relay neuron model parameters. Furthermore, analytic bounds from (16) contain results obtained through simulation of the 3rd order models of a relay neuron. Our bounds captured reliability under both the depolarized and hyperpolarized (not shown due to limited space) states of the 3rd order neuron and shows the generality of our analysis.

REFERENCES

Agarwal R. and Sarma S. V. (2011). The effects of dbs patterns on basal ganglia activity and thalamic relay. *J Comput Neurosci*, (accepted for publication).

Bekisz M. and Wrobel A. (1999). Coupling of beta and gamma activity in corticothalamic system of cats attending to visual stimuli. *NeuroReport*, 10:3589–94.

Erwin E., Baker F. H., Busen W. F., and Malpeli J. G. (1999). Relationship between laminar topology and retinotopy in the rhesus lateral geniculate nucleus: results from a functional atlas. *J.Comp neurol*, 407:92–102.

FitzHugh R. (1955). Mathematical models of threshold phenomena in the nerve membrane. *Bulletin of Mathematical Biology*, 17(4):257–278.

Greenstied Charles M. and Snell J. Laurie (2003). *Introduction to Probability*. American Mathematical Society.

Guillery R. W. and Sherman S. M. (2002). Thalamic relay functions and their role in corticocortical communication: Generalizations from the visual system. *Neuron*, 33:163–176.

Guo Y., Rubin J. E., McIntyre C. C., Vitek J. L., and Terman D. (2008). Thalamocortical relay fidelity varies in deep brain stmulation protocols in data-driven computational models. *J. Neurophysiol.*, 99:1477–1492.

Hirsch J. C., Fourment A., and Marc M. E. (1983). Sleeprelated variations of membrane potential in the lateral geniculate body relay neurons of the cat. *Brain Research*, 259(2):308–312.

Hughes S. W., Lorincz M., Cope D. W., Blethyn K. L., Kekesi K. A., Parri H. R., Juhasz G., and Crunelli V. (2004). Synchronized oscillations at α and θ frequencies in the lateral geniculate nucleus. *Neuron, Vol. 42, 253268, April 22, 2004,*.

Kastner S., Schneider K. A., and Wunderlich K. (2006). Chapter 8 beyond a relay nucleus: Neuroimaging

views on the human lgn. *Progress in Brain Research*, 155 Part B:125–143.

Lagier Samuel , Carleton Alan, and Lledo Pierre-Marie (2004). Interplay between local gabaergic interneurons and relay neurons generates γ oscillations in the rat olfactory bulb. *The Journal of Neuroscience*, 24(18):4382–4392.

Lodish H., Berk A., and Zipursky S. L. (2000). *Molecular Cell Biology. 4th edition.* W. H. Freeman.

Logothetis N. K. (2002). The neural basis of blood oxygen level dependent functional magnetic resonance imaging signal. *Phil. Trans R. Soc. Lond B*, 357(1003-37).

Lorincz M. L., Kekesi K. A., Juhasz G., Crunelli V., and Hughes S. W. (2009). Temporal framing of thalamic relay-mode firing by phasic inhibition during the alpha rhythm. *Neuron*, 63:683–96.

Manor Y., Rinzel J., Segav I., and Yarom Y. (1997). Low amplitude oscillations in inferior olive: A model based on electrical coupling of neurons with heterogeneous channel densities. *J. Neurophysiol.*

Masson G. L., Masson S. R. L., D., and Bal T. (2002). Feedback inhibition controls spike transfer in hybrid thalamic circuits. *Nature*, 417:854–858.

O'Connor D. H., Fukui M. M., Pinsk M. A., and Kastner S. (2002). Attention modulates responses in the human lateral geniculate nucleus. *nature neuroscience*, 5(11):1203–1209.

Platkiewicz J. and Brette R. (2010). A threshold equation for action potential initiation. *PloS Comput Biol*, 6(7):1000850.

Reinagel P., Godwin D., Sherman M., and Koch C. (1999). Encoding of visual information by lgn bursts. *Journal of Neurophysiology*, 81:2558–69.

Rubin J. and Josic K. (2007). The firing of an excitable neuron in the presence of stochastic trains of strong synaptic inputs. *Neural Computation*, 19:1251–1294.

Rubin J. E. and Terman D. (2004). High frequency stimulation of the subthalamic nucleus eliminates pathological thalamic rhythmicity in a computational model. *J. Comput. Neurosci.*, 16(3):211–35.

Seki Kazuhiko, Perlmutter Steve I., and Fetz Eberhard E. (2003). Sensory input to primate spinal cord is presynaptically inhibited during voluntary movement. *Nature Neuroscience*, 6:1309–1316.

Sherman S. M. (2007). The thalamus is more than just a relay. *Current Opinion in Neurobiology*, 17(4):417–422.

Sherman S. M. and Guillery R. W. (1998). On the actions that one nerve can have on another: Distinguishing "drivers" from "modulators". *PNAS*, 95(12):7121–26.

Sherman S. M. and Guillery R. W. (2002). The role of the thalamus in the flow of information to the cortex. *Phil. Trans. R. Soc. Lond. B.*, 357(1428):1695–1708.

Sohal V. and Huguenard J. (2002). Reciprocal inhibition controls the oscillatory state in thalamic networks. *Neurocomp*, 44:653–659.

Sohal V., Huntsman M., and Huguenard J. (2000). Reciprocal inhibitory connections regulate the spatiotemporal properties of intrathalamic oscillations. *J Neurosci*, 20:1735–1745.

Wolfart J., Debay D., Masson G. L., Destexhe A., and Bal T. (2005). Synaptic background activity controls spike transfer from thalamus to cortex. *Nature Neuroscience*, 8(12):1760–1767.

Zhan X., Cox C., Rinzel J., and Sherman S. (1999). Current clamp and modeling studies of lowthreshold calcium spikes in cells of the cats lateral geniculate nucleus. *J. Neurophysiol*, 81:2360–2373.

APPENDIX

Table 1: Parameters and functions for (1).

$m_\infty(V)$	$\frac{1}{(1+exp(-(V+37)/7))}$
$p_\infty(V)$	$\frac{1}{(1+exp(-(V+60)/6.2))}$
$\tau_h(V)$	$\frac{1}{0.128exp(-\frac{46+V}{18})+4/(1+exp(-\frac{23+V}{5}))}$
$h_\infty(V)$	$\frac{1}{(1+exp((V+41)/4))}$
$r_\infty(V)$	$\frac{1}{(1+exp((V+84)/4))}$
$\tau_r(V)$	$0.4(28+exp((V+25)/(-10.5)))$
V_{syn}, V_{Na}	$-85, 50mV$
V_K, V_L, V_T	$-90, -70, 0mV$
g_{Na}, g_K	$3, 5$
g_L, g_T	$0.05, 5$